Assessing single upconverting nanoparticle luminescence by optical tweezers

P. Rodríguez-Sevilla[‡], H. Rodríguez-Rodríguez[‡,†], M. Pedroni[§], A. Speghini[§], M. Bettinelli[§], J. García Solé[‡], D. Jaque[,‡], and P. Haro-González[‡]*

‡ Fluorescence Imaging Group, Departamento de Física de Materiales, Modulo 4, Universidad Autónoma de Madrid C/Francisco Tomás y Valiente 7, Madrid, 28049, Spain

§ Dipartimento di Biotecnologie, Università di Verona and INSTM, UdR Verona, Ca' Vignal, Strada Le Grazie 15, I-37134 Verona, Italy

ABSTRACT: We report on stable, long-term immobilization and localization of a single colloidal Er^{3+}/Yb^{3+} codoped upconverting fluorescent nanoparticle (UCNP) by optical trapping with a single infrared laser beam. Contrary to expectations, the single UCNP emission differs from that generated by an assembly of UCNPs. The experimental data reveal that the differences can be explained in terms of modulations caused by radiation-trapping, a phenomenon not considered before but this work reveals to be of great relevance.

KEYWORDS: Upconverting nanoparticle, optical tweezers, single particle fluorescence.

Rare earth doped luminescent nanoparticles are nowadays considered as fundamental building blocks in biophotonics applications ranging from imaging to therapy.[1, 2] Their popularity stems from their attractive and unique combination of optical properties such as reduced emission bandwidths and long luminescence lifetimes (which are independent of particle size and concentration), absence of undesirable blinking effects, high physical and chemical stability, high damage threshold and low cytotoxicity.[2, 3] Some of the rare earth doped luminescent nanoparticles can undergo a multiphoton excitation process whereby two (or more) low-energy infrared photons are sequentially absorbed and converted into higher energy photons in the visible region of the spectrum, in a process known as upconversion (UC).[4, 5] The Lanthanide-doped upconverting nanoparticles (UCNPs) demonstrate significant advantages over other traditionally used multiphoton excited probes (Semiconductor Quantum Dots and Gold nanoparticles), such as the possibility of performing multiphoton fluorescence imaging experiments with cost-effective continuous wave laser sources instead of expensive mode locked femtosecond lasers.[6, 7] In addition, the absence of "on–off" blinking in the luminescent signal made possible the use of UCNPs for single-molecule detection under near infrared (NIR) multiphoton excitation with light intensity requirements similar to those typically used for standard one-photon confocal imaging.[8, 9] Moreover, the use of NIR excitation also minimizes photodamage in biological tissues and cells and reduces the background contribution of autofluorescence. As a result of all these advantages, it is possible to find out in the literature numerous demonstrations of the potential application of UCNPs for both in vitro and in vivo high contrast imaging as well as for biodetection and biosensing applications.[3, 10-13] Indeed, UCNPs are becoming one of the most interesting nanosized luminescent probes and a careful bibliographic research revealed that almost 10 % of all the papers published in the literature dealing with the use of fluorescent nanoparticles for

bioimaging are involving them. In many of these applications, local information of the biosystem under study is obtained after a detailed spectral analysis of the luminescence generated by UCNPs. This is the case, for instance, of intracellular thermal sensing experiments, in which the cell´s temperature is obtained from the spectral analysis of the Er^{3+} ion emission of Er/Yb codoped UCNPs incorporated in living cells.[14-16] Thus, the spectral shape of Er^{3+} ion emission must be carefully investigated. In the past, optical characterization of UCNPs has been mainly limited to ensemble-averaged measurements performed either on stable colloidal suspensions or in powder samples. Nevertheless, in many real applications (intracellular imaging and tracking, and sensing) the collected luminescence is expected to be generated by a single or few UCNPs. Consequently, a complete understanding of the single UCNP luminescence is required. Assessing single UCNP emission is not only interesting from a practical point of view but also from a fundamental one. Differences between emission spectra generated by a single UCNP and an ensemble of them (already demonstrated to exists in quantum dots and gold nanoparticles) could be used to elucidate on the presence of particle-particle interactions.[17, 18]

Single UCNP emission has been reported by different groups that managed to achieve the upconverting emission spectrum of individual Er/Yb copdoped UCNPs.[19-22] In these cases particle immobilization was achieved by drop casting a diluted suspension of UCNPs on a solid substrate, in such a way those UCNPs under study were in an open air environment. These pioneering investigations pointed out the potential use of UCNPs as single-particle imaging probes due to the large signal-to noise ratio obtained in the single particle emission spectrum. Nevertheless, for most of bioapplications, the interest falls on assessing the single UCNP emission in a colloidal suspension (i.e. in an aqueous medium). Note that this is of crucial importance as several works have already pointed

out a possible dependence of UCNP luminescence on their surrounding environment.[23-25] In fact, the measurement of the luminescence spectrum generated by a single UCNP suspended in water is a challenging task. It implies the remote immobilization of a single UCNP that, otherwise, would move randomly (Brownian motion) and, thus, will be continuously escaping from the excitation beam. As an example, a single 10 nm object diffuses in water through a typical excitation spot of ≈0.3 μm in diameter in a time scale of milliseconds. Thus, additional mechanisms must be used to retain UCNP inside the excitation spot since accurate single particle emission requires observation times as long as possible to extract maximal information. Indeed, the difficulties to immobilizing an individual UCNP for long periods of time in a colloidal suspension is the main obstacle that should be overcome in order to access single UCNP emission.

Optical trapping (OT) has been demonstrated to be an accurate technique to achieve precise three dimensional translational and rotational control of single particles suspended in air or liquids. OT has been extensively used for remote manipulation of micro and nanosized objects with potential application in several areas, ranging from biology to nanophysics.[26-31] The ability of tightly focused laser beams for trapping and handling of suspended particles was pioneered by Ashkin in the 1970s.[32, 33] For nanosized particles, single beam trapping is based on the light field induced particle polarization. A nanosized particle then behaves as a dipole within a non-homogeneous electric field, so that it is attracted towards the beam focus by the so-called gradient force. In addition, a scattering force results from momentum transfer to the particle when the light is scattered by it. Under proper conditions, the gradient force can balance the scattering and gravity forces, so that the particle is retained at the laser focus.[34-37] The magnitude of the net optical force strongly depends on the polarizability of the trapped particle. Although OT has been demonstrated to nicely works with plasmonic nanoparticles, recently it has been reported

to be also applicable to the three dimensional control of dielectric nanoparticles.[30, 34-36] In particular, three dimensional remote manipulation of UCNPs has been recently demonstrated with optical forces in excess of 30 fN for laser trapping powers of 60 mW.[38] Those results provided new avenues for stable immobilization of colloidal UCNPs and, thus, opened the possibility of assessing the single UCNP emission in an aqueous environment.

In this work, we have demonstrated long term (minutes) optical trapping of a single $SrF_2:Er^{3+},Yb^{3+}$ UCNP (8 nm in size) by using a 980 nm trapping laser wavelength. The laser beam has the double function of creating the required optical force field and of exciting, via a two photon process, the visible luminescence of a single UCNP particle at the optical trap. Appropriate coupling of the single beam optical trap to a high resolution spectrometer has made possible the spectral analysis of the Er^{3+} ion red emission generated by a spatially isolated UCNP. Then the single particle emission spectrum has been compared to that obtained from an assembly of particles revealing remarkable differences that have been tentatively explained in terms of the basic absorption/emission properties of individual UCNPs.

The $SrF_2:Er^{3+},Yb^{3+}$ UCNPs used in this work were synthetized by the hydrothermal method. Details about the synthesis procedure can be found in Section S1 of Supporting Information.[12, 39] Figure 1a shows a Transmission Electron Microscopy (TEM) image of the synthesized UCNPs that present an average size of 8 nm, as can be obtained from the size dispersion histogram shown in Figure 1b. The UCNPs were dispersed in D_2O (instead of H_2O in order to avoid undesired 980 nm laser-induced heating effects),[38] showing excellent colloidal properties without evidence of precipitation during months. Recent works demonstrate the possibility of tailoring the optical forces acting on $SrF_2:Er^{3+},Yb^{3+}$ UCNPs by adequate choice of Z potential via surface modification.[40] In this work we used

UCNPs with Z potential values close to -20 mV (Figure 1c), as they lead to moderately low optical trapping forces and, hence, to reduced trapping rates (number of nanoparticles incorporating into the trap per unit of time). OT experiments were performed by the simple single beam optical tweezers setup depicted in Figure 2a that is described in detail in Section S1 of Supporting Information. Briefly, a single 980 nm laser beam was focused into a microchannel containing the colloidal suspension of UCNPs by using a high numerical aperture microscope objective. The visible emission generated by UCNPs entering the optical trap was collected by the same objective and simultaneously imaged by a CMOS camera and spectrally analyzed by a high sensitivity-high resolution spectrometer. The UCNP visible emission is generated by Er^{3+} ions excited via an efficient $Yb^{3+} \rightarrow Er^{3+}$ energy transfer process, as it has been extensively described in previous works.[5] In this work, we have focused our attention on the red emission band corresponding to the $^4F_{9/2} \rightarrow {}^4I_{15/2}$ transition of Er^{3+} ions, because of its high intensity that ensured the acquisition of high signal-to-noise luminescence spectra with moderate accumulation times (tens of seconds). Under our experimental conditions, the characteristic green emission $^2H_{11/2};{}^4S_{3/2} \rightarrow {}^4I_{15/2}$ was found to be several times weaker than the red one, so that the acquisition of high signal-to-noise ratio green emission spectra was not possible in our experimental setup (see Figure S1 in Supporting Information). For single particle trapping experiments, the concentration of UCNPs in the colloidal suspension was decreased until the average distance between UCNPs was set to be close to 10 μm, reaching a value of approximately 2 $x10^8$ NP/cm^3. Such low concentration is required in order to avoid multiple-particle trapping as well as UCNP agglomeration. Long term single UCNP trapping is experimentally demonstrated in Figure 2b that shows the time evolution of the visible emission generated at the optical trap as obtained with a 40 mW laser power. A clear rise in the emission intensity is

observed, denoting the incorporation of a single UCNP into the trap. After UCNP incorporation, the emission intensity remains constant for more than two minutes, evidencing no incorporation of a second UCNP. During this time, UCNP was immobilized at the trap position with a net force proportional to the laser trapping power (inset in Figure 2b). A trapping force close to 2 fN was obtained for a laser power of 40 mW, as determined by the hydrodynamic drag method (see Section S1 in Supporting Information) and by considering the possible influence of Faxen´s correction (as described in Section S3 in Supporting Information).[41] These optical forces were found to be strong enough to induce a controlled translation of the single UCNP by acting on (moving) the trapping beam. Figure 2c shows a sequence of pictures showing a single UCNP being moved along a square trajectory at a speed of 0.4 μm/s. Experimental results included in Figure 2 evidence that an appropriate choice of UCNP concentration and trapping beam power allows for single particle trapping and manipulation for times in excess of minutes.

The long-period trapping of a single UCNP demonstrated in Figure 2 allowed us for accessing to the single particle emission spectrum despite of its weakness. Particle immobilization during minutes allowed for the acquisition of emission spectra requiring integration times of tens of seconds. The luminescence spectrum of a single UCNP immobilized into the trap is shown in Figure 3 (red line). It is characterized by a band emission extending from 640 up to 680 nm, reaching its maximum intensity at 649 nm. As previously mentioned, this emission band is ascribed to the $^4F_{9/2} \rightarrow {}^4I_{15/2}$ transition of Er^{3+} ions that are excited by 980 nm radiation through an $Yb^{3+} \rightarrow Er^{3+}$ energy transfer upconversion process.[8] The intensity and shape of this emission spectrum was found to be highly stable, provided that no additional UCNP, were incorporated into the trap. Although appearing in the expected spectral range, the shape of the single particle

emission was found to differ from the typical emission spectrum obtained from a colloidal suspension of UCNPs when optically excited by the non-tightly focused 980 nm laser beam. Blue line in Figure 3 corresponds to the multiple-particle emission spectrum generated by a colloidal suspension of UCNPs at a concentration of 10^{15} NP/cm^3, in which a 980 nm laser beam had been focused with a 0.25 NA microscope objective (leading to an excitation spot radius of 3 μm). As can be observed, the multiple-particle emission spectrum generated by the colloidal suspension of UCNPs shows a band also extending from 640 up to 680 nm with two main emission peaks centered at about 650 nm and 665 nm of comparable intensities. At this point, it is important to mention that we systematically measured the emission spectra of colloidal suspensions with different concentrations. Under our experimental conditions, the minimum UCNP concentration that provided a measurable emission spectrum was found to be 10^{13} NP/cm^3 and, hence, to an UCNP-UCNP average distance of 300 nm. Even for this low concentration, the emission spectrum of the colloidal suspension does not show relevant differences to that included in Figure 3 (see Figure S2 in the Supporting Information). The emission spectra in Figure 3 were both obtained with the same detection system so that the differences could not be attributed to any experimental artifact. Indeed, these spectral differences should arise from the different UCNP-UCNP interaction processes. Such differences can be understood by taking into account the work recently published by Sarkar et al.[42] In that work, authors demonstrated that inter-particle non-radiative energy transfer between small colloidal rare-earth doped nanoparticles is mainly governed by the existence of particle-particle collisions. Thus, it was postulated that the magnitude of inter-particle interaction depends not on the average distance between particles but, instead, on the collision rate between colloidal nanoparticles. The collision rate between UCNPs, although difficult to evaluate, would increase with the number of optically trapped

UCNPs. Thus, accordingly with Sarkar et al.,[42] the magnitude of inter-particle interaction would be also expected to increase with the number of optically trapped UCNPs. This will be increase the non-radiative and radiative energy transfer rates between Er^{3+} ions. While non-radiative transfer does not produce spectral shape changes, the radiative one would modify the shape of the Er^{3+} emission band. In other words, the Er^{3+} ions emission spectrum obtained during controlled incorporation of individual UCNPs into the trap should reveal a gradual spectral change from the single particle to the multi-particle emission spectrum. Controlled incorporation of individual UCNPs into the trap could be achieved by performing trapping experiments with larger trapping powers. Sequential UCNP incorporation into a 70 mW laser power trap is evidenced by the emission intensity profile included in Figure 4a in which each intensity step corresponds to the incorporation into the trap of an additional UCNP (process also schematically illustrated in Figure 4a). Under these experimental conditions, we estimated that the UCNP incorporation rate into the trap was 1 UCNP every 20 seconds, i.e 0.05 particles/s. Figure 4b shows the emission spectra measured during this sequential incorporation with an integration time interval of 30 seconds (this being the integration time required for low noise spectrum acquisition). During the initial 30 seconds, only one UCNP was present in the optical trap and the recorded spectrum is dominated by the emission line at 649 nm, in good agreement with the single particle emission spectrum included in Figure 3 (obtained with a reduced laser trapping power of 40 mW). As time goes by, UCNPs are sequentially incorporated into the trap that leads to an increment in the particle-particle collision rate. Since the position histogram of a trapped particle is complex,[43] in this work we did not attempt to evaluate such collision rate but, instead, we just discuss experimental data in terms of the number of optically trapped UCNPs (by considering a constant incorporation rate into the trap of 0.05 NP/s). Figure 5 includes the estimated number of optically trapped UCNPs as a

function of the trapping time. The ratio between emitted intensities at 665 nm and 649 nm is found to increase continuously with time up to a saturation value (gray dots in Figure 5). This means that this ratio increases with the number of UCNPs inside the trap, i.e. with the inter-particle collision rate. Regarding the saturation value, it is important to remind here that the I_{665}/I_{649} emission intensity ratio obtained from a colloidal suspension of UCNPs corresponds to 0.82. Thus, it should be noted that about 2.5 minutes after trapping started, the I_{665}/I_{649} intensity ratio starts to saturate at 0.82 indicating that, for this trapping time, the trap emission spectrum resembles that of the colloidal suspension (Figure 4b). At this time (2.5 minutes after trapping starts), we estimate that up to 7 UCNPs had entered the trap.

Experimental data included in Figure 4 and 5 evidence the existence of a transition from single-particle to multi-particle fluorescence in our colloidal UCNPs causing relevant changes in the spectral shape of the red Er^{3+} ions emission. At this point, we postulate inter-particle collision assisted radiative trapping (or self-absorption) as the UCNP-UCNP interacting mechanism causing the observed spectral changes.[44-46] To support this statement, figure 6a shows the room temperature absorption and emission spectra of a colloidal suspension of UCNPs (10^{15} NP/cm^3) in the red spectral region. The spectral overlap between absorption and emission bands is evident. From a proper analysis of emission and absorption spectra, the lineshape functions ($g_E(\upsilon)$ and $g_A(\upsilon)$ for emission and absorption, respectively) can be calculated. Results are included in Section S5 of Supporting Information from which an spectral overlap of $\int g_A(\upsilon)\, g_E(\upsilon) d\upsilon = 4.6 \times 10^{-14}$ s^{-1} has been obtained, this being close to three times larger than the spectral overlap obtained for the green emission of Er^{3+} ions ($^2H_{11/2}$;$^4S_{3/2} \rightarrow {}^4I_{15/2}$) (Section S5 in Supporting Information). Note that the existence of a non-negligible overlap between absorption and emission lineshape functions was, nevertheless, expected. From Figure

6a, it is clear that self-absorption of red emission would be especially relevant for emitted photons with wavelength close to 650 nm, where maximum overlap occurs. In fact, the terminal level of the radiative decay is the $^4I_{15/2}$ ground state of Er^{3+} ions (Figure 6b) in such a way that emitted photons can be partially re-absorbed, and so promoting electronic back-excitations from the ground up to the $^4F_{9/2}$ emitting state. As a result, in presence of this self-absorption process, the red emission spectrum ($^4F_{9/2} \rightarrow {}^4I_{15/2}$ transition) would be modulated resulting in a reduction in the overall emitted intensity for wavelengths close to 650 nm. This modulation will increase as the magnitude of particle-particle interactions increase, i.e. as the trapping time increase. At the same time, the emission intensity at about 665 nm is almost unaffected by self-absorption since the overlap between absorption and emission around 665 nm is very weak (Figure 6a). Therefore, the 'pure' emission of a single UCNP (without any spectral modulation caused by self-absorption) would be only obtained in the absence of any absorbing UCNP in its surroundings, i.e. for optical trapping of a single UCNP. Under these conditions the distance between UCNPs is too large and the collision rate between UCNPs can be neglected, so that UCNP can be considered as an isolated luminescence unit and the detected luminescence exactly reproduces the single UCNP luminescence. On the contrary, when several UCNPs are incorporated into the trap, collision-assisted inter-particle interactions cannot be neglected, as reported by Sarkar et al.[42] In this case, the detected luminescence is that of a single UCNP but modulated by the absorption spectrum of collisioning (neighboring) UCNPs. As it is explained in Section S6 of Supporting Information, the basic formalism of radiative energy transfer reveals that in our particular case, such interactions become relevant only when pseudo-contact between UCNPs is produced, i.e. they require the existence of collisions between UCNPs. Pseudo-contact between optically trapped UCNPs can be produced inside the trap not only by collisions between intra-trap moving

UCNPs, but it could be also induced if UCNP aggregation is taking place. Nevertheless, we here state that intra-trap aggregation can be discarded, as agglomeration would lead to loss of colloidal character and then a precipitation of the luminescent particles out of the optical trap (a not observed effect). In addition, DLS measurements performed on colloidal dispersion with UCNP concentrations as large as 10^{14} particles/cm^3, much larger than the intra-trap particle densities achieved in our experiments, reveal that UCNPS show an hydrodynamic diameter close to 8 nm (see Figure S5 in Supporting Information). This is virtually the same as particle diameter determined by TEM (see Figure 1), indicating that "multi-particle fluorescence" does not involves particle aggregation.

In summary, we have provided experimental evidence of the relevant role that the inter-particle interactions can have in the luminescent properties of colloidal suspensions of upconverting nanoparticles. In particular, the single particle red emission of a long-period (minutes) optically immobilized SrF_2:Er^{3+},Yb^{3+} UCNP has been found to be clearly different from the multi-particle emission spectrum. Single beam optical tweezers allowed us to monitor the transition from single-particle to multi-particle fluorescence by promoting sequential particle incorporation into the trap. The remarkable differences between single and multi-particle luminescence have been explained in terms of the existence of significant collision-assisted radiative self-absorption processes between UCNPs, due to the partial overlap between absorption and emission bands.

The results provided in this work reveal that the previously reported properties of colloidal luminescent nanoparticles could have to be, in some cases, re-considered as they ignored the possible presence of particle-particle interactions that could be of relevant importance.

ASSOCIATED CONTENT

Supporting Information.

The contents of the Supporting Information are: S1.- Experimental Section. S2.- 500-700 nm emission spectrum of a colloidal suspension of SrF_2:Er^{3+},Yb^{3+} nanoparticles. S3.- Faxen´s Corrections to measured trapping forces. S4.- Emission spectra in the red range from colloidal suspensions of different UCNP concentrations. S5.- Spectral overlap calculations. S6.- Calculation of critical distances for radiative energy transfer between UCNPs. S7.- DLS experiments. This material is available free of charge via the Internet at http://pubs.acs.org.

AUTHOR INFORMATION

Corresponding Author

* E-mail: daniel.jaque@uam.es

Present Addresses

† IMDEA Nanoscience, Campus de Cantoblanco 28049, Madrid, Spain

Author Contributions

The manuscript was written through contributions of all authors. All authors have given approval to the final version of the manuscript.

ACKNOWLEDGMENT

This work was supported by the Spanish Ministerio de Educación y Ciencia (MAT2010–16161 and MAT2013–47395-C4–1-R). P.H.G. thanks the Spanish Ministerio de Economía y Competitividad (MINECO) for the Juan de la Cierva program. P.R.S thanks the Spanish Ministerio de Economía y Competitividad (MINECO) for the “Promoción

del talento y su Empleabilidad en I+D+i" statal program. Fondazione Cariverona (Verona, Italy) is gratefully acknowledged for financial support in the frame of the project "Verona Nanomedicine Initiative". The authors declare no competing financial interest.

ABBREVIATIONS

UCNP, Upconverting luminescent nanoparticle

NIR, near infrared

OT, Optical trapping

TEM, Transmission Electron Microcopy

REFERENCES

1. Wang, F.; Banerjee, D.; Liu, Y.; Chen, X.; Liu, X. *Analyst* **2010,** 135, 1839-1854.
2. Wang, F.; Liu, X. *Chem. Soc. Rev.* **2009,** 38, 976-989.
3. Chatterjee, D. K.; Gnanasammandhan, M. K.; Zhang, Y. *Small* **2010,** 6, 2781-2795.
4. Auzel, F. *Chem Rev* **2004,** 104, 139-73.
5. Auzel, F. *J. Lumin.* **1990,** 45, 341-345.
6. Ropp, C.; Cummins, Z.; Nah, S.; Fourkas, J. T.; Shapiro, B.; Waks, E. *Nat Commun* **2013,** 4, 1447.
7. Wang, F.; Han, Y.; Lim, C. S.; Lu, Y.; Wang, J.; Xu, J.; Chen, H.; Zhang, C.; Hong, M.; Liu, X. *Nature* **2010,** 463, 1061-1065.
8. Gnach, A.; Bednarkiewicz, A. *Nano Today* **2012,** 7, 532-563.
9. Ryu, J.; Park, H.-Y.; Kim, K.; Kim, H.; Yoo, J. H.; Kang, M.; Im, K.; Grailhe, R.; Song, R. *J. Phys. Chem. C* **2010,** 114, 21077-21082.
10. Wang, F.; Banerjee, D.; Liu, Y. S.; Chen, X. Y.; Liu, X. G. *Analyst* **2010,** 135, 1839-1854.
11. Deng, W.; Goldys, E. M. *Analyst* **2014,** 139, 5321-5334.
12. Dong, N. N.; Pedroni, M.; Piccinelli, F.; Conti, G.; Sbarbati, A.; Ramirez-Hernandez, J. E.; Maestro, L. M.; Iglesias-de la Cruz, M. C.; Sanz-Rodriguez, F.; Juarranz, A.; Chen, F.; Vetrone, F.; Capobianco, J. A.; Sole, J. G.; Bettinelli, M.; Jaque, D.; Speghini, A. *ACS Nano* **2011,** 5, 8665-8671.
13. Vetrone, F.; Naccache, R.; Zamarron, A.; Juarranz de la Fuente, A.; Sanz-Rodriguez, F.; Martinez Maestro, L.; Martin Rodriguez, E.; Jaque, D.; Garcia Sole, J.; Capobianco, J. A. *ACS Nano* **2010,** 4, 3254-3258.
14. Jaque, D.; Vetrone, F. *Nanoscale* **2012,** 4, 4301-4326.
15. Brites, C. D. S.; Lima, P. P.; Silva, N. J. O.; Millan, A.; Amaral, V. S.; Palacio, F.; Carlos, L. D. *Nanoscale* **2012,** 4, 4799-4829.
16. Brites, C. D. S.; Lima, P. P.; Silva, N. J. O.; Millan, A.; Amaral, V. S.; Palacio, F.; Carlos, L. D. *New J. Chem.* **2011,** 35, 1177-1183.
17. Nikoobakht, B.; El-Sayed, M. A. *J. Phys. Chem. A* **2003,** 107, 3372-3378.
18. Jassby, D.; Wiesner, M. *Langmuir* **2011,** 27, 902-908.
19. Wu, S.; Han, G.; Milliron, D. J.; Aloni, S.; Altoe, V.; Talapin, D. V.; Cohen, B. E.; Schuck, P. J. *Proc. Natl. Acad. Sci. U. S. A.* **2009,** 106, 10917-10921.
20. Gargas, D. J.; Chan, E. M.; Ostrowski, A. D.; Aloni, S.; Altoe, M. V. P.; Barnard, E. S.; Sanii, B.; Urban, J. J.; Milliron, D. J.; Cohen, B. E.; Schuck, P. J. *Nat. Nanotechnol.* **2014,** 9, 300-305.
21. Schietinger, S.; Aichele, T.; Wang, H.-Q.; Nann, T.; Benson, O. *Nano Lett.* **2010,** 10, 134-138.
22. Schietinger, S.; Menezes, L. D.; Lauritzen, B.; Benson, O. *Nano Lett.* **2009,** 9, 2477-2481.
23. Wu, T.; Wilson, D.; Branda, N. R. *Chem. Mater.* **2014,** 26, 4313-4320.
24. Hao, S.; Chen, G.; Yang, C. *Theranostics* **2013,** 3, 331-345.
25. Bogdan, N.; Vetrone, F.; Ozin, G. A.; Capobianco, J. A. *Nano Lett.* **2011,** 11, 835-840.
26. Geiselmann, M.; Juan, M. L.; Renger, J.; Say, J. M.; Brown, L. J.; de Abajo, F. J. G.; Koppens, F.; Quidant, R. *Nat Nano* **2013,** 8, 175-179.
27. Perkins, T. T. *Laser Photon. Rev.* **2009,** 3, 203-220.

28. Sacconi, L.; Tolic-Norrelykke, I. M.; Stringari, C.; Pavone, F. S. *Imaging, Manipulation, and Analysis of Biomolecules, Cells, and Tissues IV* **2006,** 6088, C881-C881.
29. Uchida, M.; Satomaeda, M.; Tashiro, H. *Curr. Biol.* **1995,** 5, 380-382.
30. Ashkin, A.; Dziedzic, J. M.; Yamane, T. *Nature* **1987,** 330, 769-771.
31. Hormeño, S.; Arias-Gonzalez, J. R. *Biology of the Cell* **2006,** 98, 679-695.
32. Ashkin, A. *Phys. Rev. Lett.* **1970,** 24, 156-159.
33. Ashkin, A.; Dziedzic, J. M.; Bjorkholm, J. E.; Chu, S. *Opt. Lett.* **1986,** 11, 288-290.
34. Bendix, P. M.; Jauffred, L.; Norregaard, K.; Oddershede, L. B. *IEEE J. Sel. Top. Quantum Electron.* **2014,** 20, 15-26.
35. Dholakia, K.; Reece, P.; Gu, M. *Chem. Soc. Rev.* **2008,** 37, 42-55.
36. Dienerowitz, M.; Mazilu, M.; Dholakia, K. *J. Nanophoton* **2008,** 2, 021875-021875.
37. Neuman, K. C.; Block, S. M. *Rev. Sci. Instrum.* **2004,** 75, 2787-2809.
38. Haro-Gonzalez, P.; del Rosal, B.; Maestro, L. M.; Rodriguez, E. M.; Naccache, R.; Capobianco, J. A.; Dholakia, K.; Garcia Sole, J.; Jaque, D. *Nanoscale* **2013,** 5, 12192-12199.
39. Pedroni, M.; Piccinelli, F.; Passuello, T.; Polizzi, S.; Ueda, J.; Haro-Gonzalez, P.; Martinez Maestro, L.; Jaque, D.; Garcia-Sole, J.; Bettinelli, M.; Speghini, A. *Cryst. Growth Des.* **2013,** 13, 4906-4913.
40. Rodríguez-Rodríguez, H.; Rodríguez Sevilla, P.; Martín Rodríguez, E.; Ortgies, D. H.; Pedroni, M.; Speghini, A.; Bettinelli, M.; Jaque, D.; Haro-González, P. *Small* **2015,** 11, 1555-1561.
41. Svoboda, K.; Block, S. M. *Annu. Rev. Biophys. Biomol. Struct.* **1994,** 23, 247-285.
42. Sarkar, S.; Meesaragandla, B.; Hazra, C.; Mahalingam, V. *Adv. Mater.* **2013,** 25, 856-860.
43. Jauffred, L.; Kyrsting, A.; Arnspang, E. C.; Reihani, S. N. S.; Oddershede, L. B. *Nanoscale* **2014,** 6, 6997-7003.
44. Mattarelli, M.; Montagna, M.; Zampedri, L.; Chiasera, A.; Ferrari, M.; Righini, G. C.; Fortes, L. M.; Goncalves, M. C.; Santos, L. F.; Almeida, R. M. *Europhys. Lett.* **2005,** 71, 394-399.
45. Sumida, D. S.; Fan, T. Y. *Opt. Lett.* **1994,** 19, 1343-1345.
46. Auzel, F.; Baldacchini, G.; Laversenne, L.; Boulon, G. *Opt. Mater.* **2003,** 24, 103-109.

TABLE OF CONTENTS

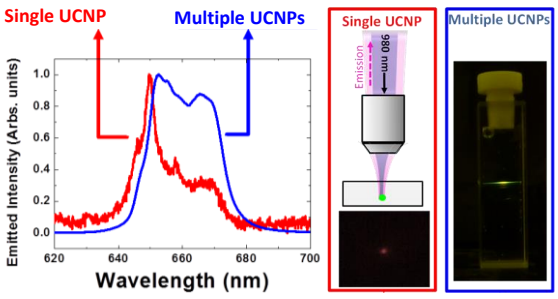

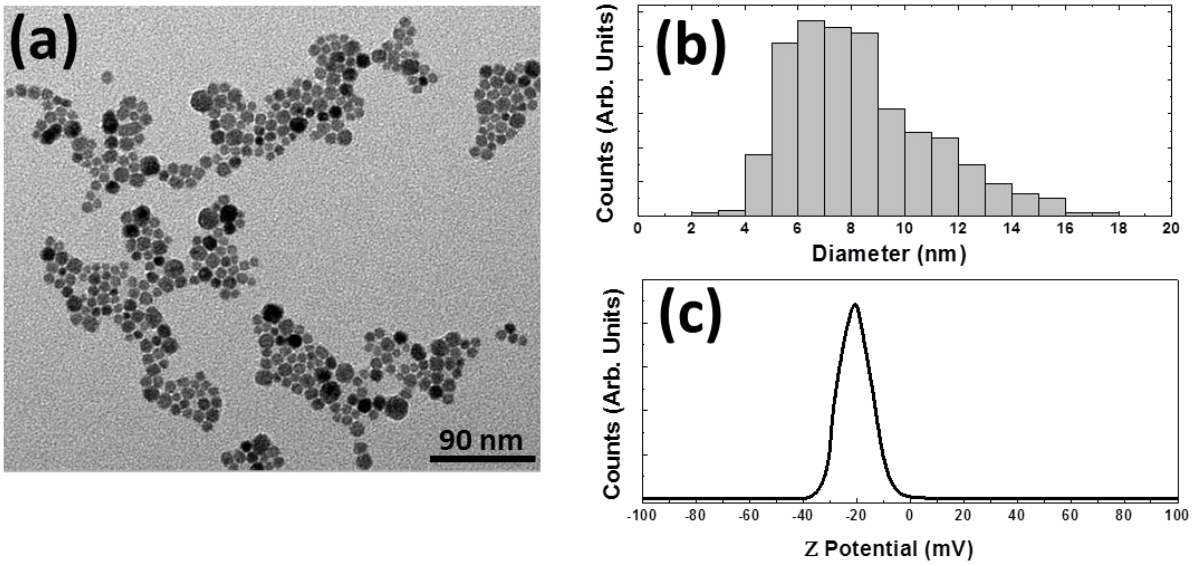

Figure 1. (a) TEM image of the UCNPs used all along this work. **(b)** Size histogram as obtained from the TEM images. **(c)** Z potential spectrum of the UCNPs used in this work.

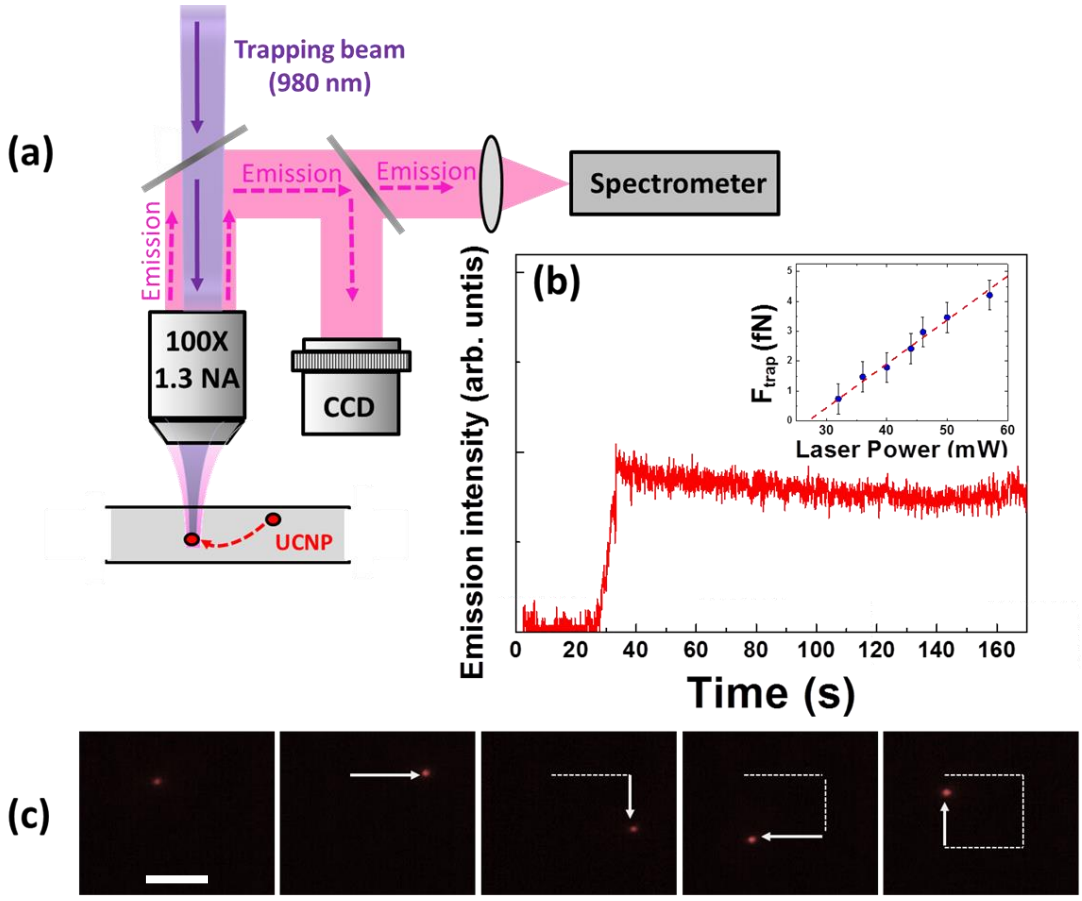

Figure 2. (a) Schematic diagram of the experimental setup used for luminescence acquisition of an optically trapped UCNP. **(b)** Time evolution of the trap luminescence, denoting the incorporation of a single UCNP. Inset shows the trapping force as a function of the laser power. Dots are experimental data and dashed line is the best linear fit. **(c)** Fluorescence image of a single optically trapped UCNP that is being translated along a square trajectory. Scale bar is 2 μm, in all the cases.

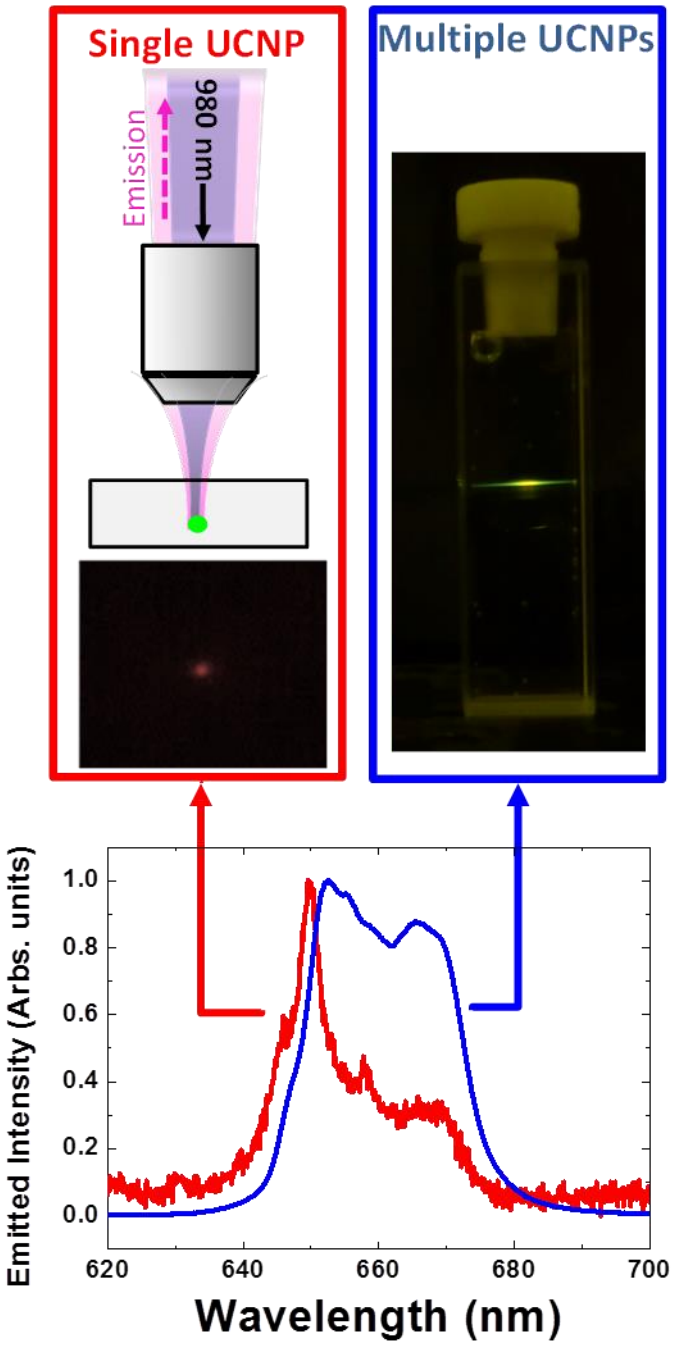

Figure 3. Upconversion emission spectra, as obtained from a single UCNP (red) and from multiple UCNPs (blue). Data were obtained from a single optically trapped UCNP and from a colloidal suspension of UCNPs (10^{15} NP/cm^3), being the last one excited with a non-tightly focused laser beam. Excitation laser wavelength was, in both cases, 980 nm.

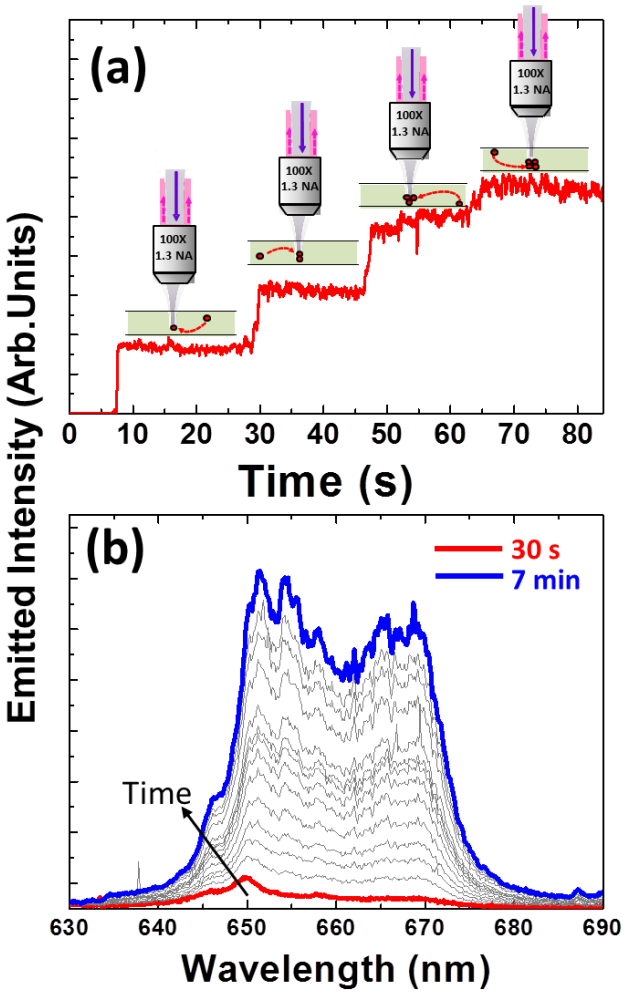

Figure 4. (a) Time evolution of the two-photon excited luminescence generated by optically trapped UCNPs. The intensity steps denote the sequential incorporation of UCNPs into the trap as it is schematically indicated in the Figure. **(b)** Emission spectra generated by optically trapped UCNPs as measured at different times in the same experimental conditions as those used in Figure 3 for single particle trapping, but with a higher laser power. Time interval between consecutive measurements was 30 s. The emission spectra obtained by a single UCNP (measured 30 s after switching on the trapping laser) and by several optically trapped UCNPs (obtained 7 min after trapping laser was switched on) are highlighted in red and blue, respectively.

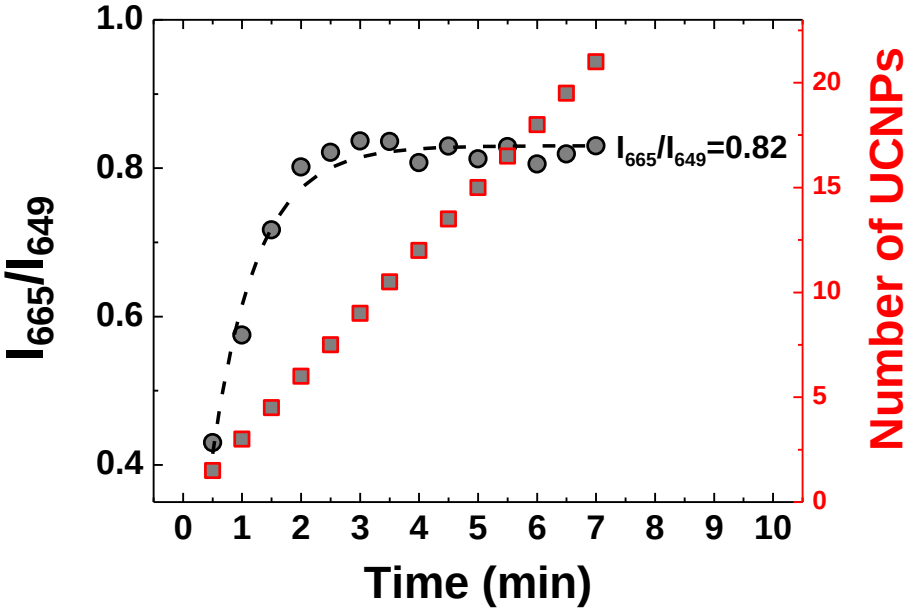

Figure 5. Ratio (gray dots) between the emitted intensities at 665 nm (I_{665}) and at 649 nm (I_{649}) as a function of the trapping time (data extracted from the emission spectra included in Figure 4b). Dashed black line is a guide for the eye. The evolution of the number of optically trapped UCNPs is included as red squares.

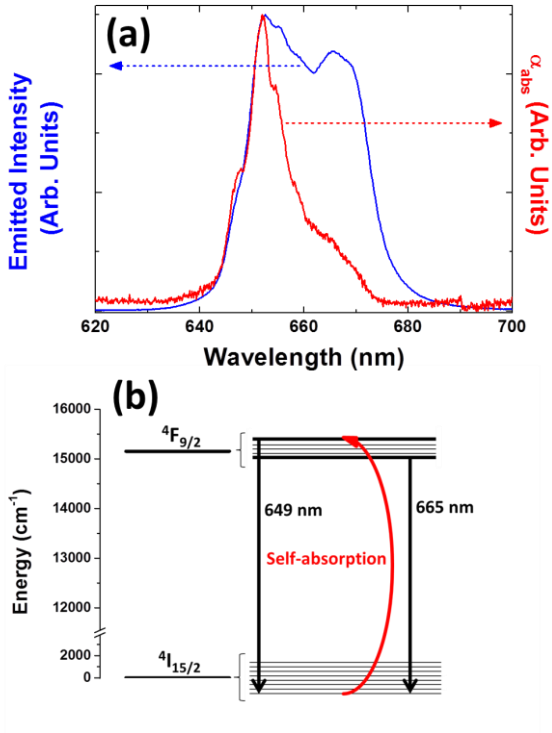

Figure 6. (a) Room temperature absorption and emission spectra of a colloidal suspension of UCNPs (10^{15} NP/cm^3). **(b)** Energy level scheme of Er^{3+} ion in the SrF_2 host. Just emission band corresponding to the $^4F_{9/2} \rightarrow {}^4I_{15/2}$ transition is shown. Both emission peaks are represented and those involved in self-absorption process are linked with a red arrow.